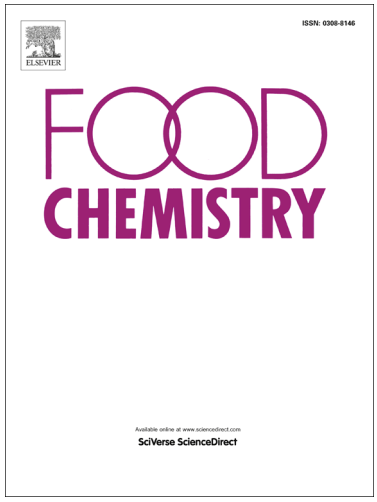

Sulfur dioxide induced aggregation of wine thaumatin-like proteins: role of disulfide bonds

Ricardo Chagas, César A.T. Laia, Ricardo B. Ferreira, Luísa M. Ferreira

PII: S0308-8146(18)30557-0
DOI: https://doi.org/10.1016/j.foodchem.2018.03.115
Reference: FOCH 22658

To appear in: *Food Chemistry*

Received Date: 23 December 2017
Revised Date: 6 March 2018
Accepted Date: 26 March 2018

Please cite this article as: Chagas, R., Laia, C.A.T., Ferreira, R.B., Ferreira, L.M., Sulfur dioxide induced aggregation of wine thaumatin-like proteins: role of disulfide bonds, *Food Chemistry* (2018), doi: https://doi.org/10.1016/j.foodchem.2018.03.115

Sulfur dioxide induced aggregation of wine thaumatin-like proteins: role of disulfide bonds

AUTHOR NAMES

Ricardo Chagas[a,b*], César A. T. Laia[a], Ricardo B. Ferreira[b], Luísa M. Ferreira[a*]

AUTHOR ADDRESSES

[a] LAQV-REQUIMTE, Departamento de Química, Faculdade de Ciências e Tecnologia, Universidade NOVA de Lisboa, Campus de Caparica, 2829-516 Caparica, Portugal

[b] LEAF, Instituto Superior de Agronomia, Universidade de Lisboa, 1349-017 Lisboa, Portugal

*corresponding authors

Highlights

- Aggregation of wine TLPs is triggered by sulfur dioxide upon cooling after a heat stress
- Wine TLPs are the most reactive to sulfur dioxide under heat stress
- Sulfur dioxide induced protein reduction and disulfide bonds scrambling
- Aggregates are held by hydrophobic interactions and intermolecular disulfide bonds

ABSTRACT

Aggregation of heat unstable wine proteins is responsible for the economically and technologically detrimental problem called wine protein haze. This is caused by the aggregation of thermally unfolded proteins that can precipitate in bottled wine. To study the influence of SO_2 in this phenomenon, wine proteins were isolated and thaumatins were identified has the most prone to aggregate in the presence of this compound. Isolated wine thaumatins aggregation was followed by dynamic light scattering (DLS), circular dichroism (CD), fluorescence spectroscopy and size exclusion chromatography (SEC). Our experimental results demonstrate that protein thermal unfolding after exposure of the protein to 70 ^{o}C does not present differences whether SO_2 is present or not. Conversely, when the protein solution is cooled to 15 ^{o}C (after heat stress) significant analytical changes can be observed between samples with and without SO_2. A remarkable change of circular dichroism spectra in the region 220-230 nm is observed (which can be related to S-S torsion angles), as well as an increase in tryptophan fluorescence intensity (absence of fluorescence quenching by S-S bonds). Formation of covalently-linked dimeric and tetrameric protein species were also detected by SEC. The ability to dissolve the aggregates with 8 M urea seems to indicate that hydrophobic interactions are prevalent in the formed aggregates. Also, the reduction of these aggregates with tris (2-carboxyethyl) phosphine (TCEP) to only monomeric species reveals the presence of intermolecular S-S bonds.

Keywords

Wine; Haze; Sulfur dioxide; Protein aggregation

Introduction

Protein aggregation is a common phenomenon and a major obstacle to handling proteins in vitro (Ciaccio & Laurence, 2009). Most proteins can be physically and chemically unstable if they are not in their optimum medium. Factors that influence the stability of a protein have been divided by Trivedi, Laurence, and Siahaan (2009) in two categories: (1) intrinsic factors, derived from the inherent physicochemical properties of the protein itself, and (2) extrinsic factors, derived from the environment where the protein is located, such as pH, temperature, ionic strength and excipients. These factors may affect disulfide (SS) bonds and SS bond reshuffling has been proposed as having a high impact on protein aggregation. Newly formed intramolecular bonds resulting from the SS bonds reshuffling change protein conformation, whereas intermolecular bonds change the resulting particle molecular weight (Rombouts, Lagrain, Scherf, Lambrecht, Koehler, & Delcour, 2015).

New SS bond formation or SS reshuffling was already described to occur during food processing which often includes heating steps (Van der Plancken, Van Loey, & Hendrickx, 2005). Some examples of these reactions include the aggregation of milk β-lactoglobulin after heating (where formed aggregates are held together by a mixture of intermolecular non-covalent association and heat-induced non-native disulfide bonds) or the aggregation of egg white proteins after heat and pressure treatments (where the formation of aggregates is caused by SH-SS exchange, SH oxidation and increased hydrophobic interactions among proteins) (Creamer, Bienvenue, Nilsson, Paulsson, van Wanroij, Lowe, et al., 2004; Van der Plancken, Van Loey, & Hendrickx, 2005).

One of the food industries typically affected by this type of problem is the wine industry. A wine can turn turbid during inappropriate storage or transportation due the insolubilization and aggregation of residual proteins that remain in wine after the

fermentation process, a phenomenon commonly known as protein haze (Batista, Monteiro, Loureiro, Teixeira, & Ferreira, 2009). Formation of these unattractive precipitates in bottled wine is a common defect of commercial white wines, making them unacceptable for sale. For this reason, guaranteeing wine stability prior to bottling is an essential step of the winemaking process, and presents a significant challenge for winemakers (Van Sluyter, McRae, Falconer, Smith, Bacic, Waters, et al., 2015). Protein haze formation in wine has been described and studied for over 30 years, with incidence not only on the characterization of stable/unstable wine proteins but also on the mechanism of formation of protein haze in white wine (Chagas, Ferreira, Laia, Monteiro, & Ferreira, 2016; Hsu & Heatherbell, 1987; Van Sluyter, et al., 2015). This phenomenon has been described as a multi-factorial process since several components of the wine matrix other than the proteins themselves also contribute to haze formation. These components comprise some wine constituents such as organic acids, sulfate, polyphenols and polysaccharides and other factors such as the pH or ionic strength of the medium (Batista, Monteiro, Loureiro, Teixeira, & Ferreira, 2010; Ferreira, Piçarra-Pereira, Monteiro, Loureiro, & Teixeira, 2001; Jaeckels, Meier, Dietrich, Will, Decker, & Fronk, 2016; Pocock, Alexander, Hayasaka, Jones, & Waters, 2007). The interaction of these components, and other wine metabolites, with different isolated wine proteins was extensively studied by dynamic light scattering (DLS), circular dichroism (CD), fluorescence spectroscopy, among other techniques (Chagas, Lourenco, Monteiro, Ferreira, & Ferreira, 2017; Di Gaspero, Ruzza, Hussain, Vincenzi, Biondi, Gazzola, et al., 2017; Dufrechou, Poncet-Legrand, Sauvage, & Vernhet, 2012; Dufrechou, Vernhet, Roblin, Sauvage, & Poncet-Legrand, 2013; Marangon, Sauvage, Waters, & Vernhet, 2011).

More recently, Van Sluyter, et al. (2015) presented a revised scheme of the possible protein haze formation mechanism. A significant input to this revised mechanism was

the solution of the crystal structure of wine isolated thaumatin-like proteins (TLP) by which unstable isoforms of TLPs were shown to have an exposed loop stabilized by a disulfide bridge that can be destabilized by heat (Marangon, Van Sluyter, Waters, & Menz, 2014). Although it was hypothesized that the aggregation of these isoforms can be exacerbated under conditions that favor disulfide bond reduction, their aggregation was only tested for the presence of sulfate during a heat test. In parallel, Chagas, Ferreira, Laia, Monteiro, and Ferreira (2016) identified sulfur dioxide as the critical factor influencing the haze potential of the main fraction of wine proteins in model wine solution. The interaction of sulfur dioxide with wine proteins under real conditions was also validated by the same authors. Sulfur dioxide is a common preservative in the food industry and the most important chemical compound widely used by the wine industry due to its antiseptic and antioxidant properties (Garde-Cerdán, López, Garijo, González-Arenzana, Gutiérrez, López-Alfaro, et al., 2014). A direct relation was demonstrated between the haze potential of some of the isolated fractions of wine proteins and the SO_2 content of the medium, with higher protein aggregation in samples containing higher SO_2 levels (Chagas, Ferreira, Laia, Monteiro, & Ferreira, 2016). Although the participation of SO_2 on the development protein aggregates was confirmed, the possible formation of new interprotein disulphide bounds was not analytically validated.

The present work aimed the elucidation of the molecular steps by which isolated wine proteins evolve from soluble to aggregated, in model wine solution, after heat stress in the presence of sulphur dioxide. To this end, proteins were isolated and identified, and their aggregation progress was followed by different techniques.

Materials and methods

Materials

Total wine protein was purified from a varietal Moscatel of Alexandria white wine, 2014 vintage, from Instituto Superior de Agronomia, Lisbon, Portugal. The used model wine solution (MWS) consisted of 12% (v/v) ethanol, 5 g/L tartaric acid and pH adjusted to 3.2.

A ratio of 100 mg L^{-1} of protein for 120 mg L^{-1} of total SO_2 was considered as a concentration similar to that often found in wines (Chagas, Ferreira, Laia, Monteiro, & Ferreira, 2016). This ratio was used in the spectrofluorimetry trial, though for the remaining trails the protein concentration was increased to increment the signal intensity. To this end, both protein and SO_2 concentrations were increased 5-fold, to a final protein concentration of 500 mg L^{-1} and a total SO_2 final concentration of 600 mg L^{-1}. Sulfur dioxide was always added as $NaHSO_3$ (Merck, Darmstadt, Germany).

Reagents

Sodium hydroxide, hydrochloric acid and sodium chloride were obtained from Panreac (Barcelona, Spain). Sodium hydrogen sulfite, sodium citrate, citric acid, ammonium sulfate and potassium phosphate were acquired from Merck (Darmstadt, Germany). Poly(vinylpolypyrrolidone) (PVPP), 5,5′-dithiobis (2-nitrobenzoic acid) (DTNB), urea, 2-amino-2-(hydroxymethyl)-1,3-propanediol hydrochloride (Tris-HCl), bovine serum albumin (BSA), cytochrome *c*, trichloroacetic acid (TCA) and *meso*-Tartaric acid monohydrate were purchased from Sigma–Aldrich (Steinheim, Germany).

Protein purification

Wine total protein was isolated as described previously (Chagas, Ferreira, Laia, Monteiro, & Ferreira, 2016; Marangon, Van Sluyter, Haynes, & Waters, 2009) with some modifications. The wine sample was adjusted to pH 3.0 with HCl and treated with 30 g/L of PVPP overnight at 4 °C. The wine was vacuum filtered through three layers of Miracloth (Merck, Darmstadt, Germany) followed by two filtrations through polyethersulfone (PES) filters (0.45 and 0.22 μm). All chromatographic steps were executed at room temperature. Using the ÄKTA Pure pump, filtered wine was loaded at 5 mL/min onto a RESOURCE S column (6 mL, Amersham Biosciences) previously equilibrated with 30 mM sodium citrate, pH 3.0. The column was then connected to an ÄKTA Pure chromatography system with UV detector (Amersham Biosciences) and washed at 6 mL/min with 10 column volumes of 30 mM sodium citrate, pH 3.0. Bound proteins were eluted at 6 mL/min with 30 mM sodium citrate, 1 M NaCl, pH 3.0 (buffer B) using the following gradient: 0 mL, 0% B; 30 mL, 50% B; 60 mL, 100% B and held. The protein fraction was desalted on PD-10 columns (GE Healthcare), lyophilized and stored at -20 ºC until use. Before use, the sample was thawed and dissolved in 50 mM sodium citrate containing 1.25 M ammonium sulfate, pH 3.0, and loaded on a Phenyl Superose HR 5/5 HIC column (GE Healthcare). After each injection, the column was washed with 6 mL of 50 mM sodium citrate, pH 3.0, containing 1.7 M ammonium sulfate. Bound proteins were eluted at 0.5 mL/min with a 30 mL gradient to 50 mM sodium citrate, pH 3.0. Fractions were pooled based on absorption profiles at 280 nm, desalted in PD-10 columns, lyophilized and stored at -20 °C until use.

Heat test

Samples were heated at 80 ºC for 2 h in a thermomixer and subsequently cooled in ice for 2 h. After equilibration at room temperature, the increase in turbidity was detected spectrophotometrically at 540 nm. Differences in wine turbidity (before and after heat treatment) have been shown to correlate directly to wine protein instability (Marangon, Stockdale, Munro, Trethewey, Schulkin, Holt, et al., 2013). All measurements were performed in triplicate.

Determination of protein sulphydryl content (DTNB assay)

Determination of SH-group content in proteins was performed following the DTNB assay described by Shimada and Cheftel (1989) with some modifications. Since there was the need to solubilize the protein aggregates to perform the DTNB assay, the buffers used in the standard method were adapted. All samples were treated equally except the heat stressed samples that were subjected to a heat test prior to the DTNB assay. A summary of the modification of the DTNB trial is described below.

DTBN assay of protein not subjected to heat stress

Isolated wine protein (D from HIC, Fig. S1B) was dissolved in water at a concentration of 50 µM. To 250 µL of protein solution, 250 µL of Buffer D (Tris-HCl 200 mM, SDS 4% w/v, pH 8) was added, for a protein final concentration of 25 µM. Samples to be reduced were added of 0.88 µL of 2-mercaptoethanol. After equilibration for 1 h at 25 ^{o}C, proteins were precipitated by adding trichloroacetic acid (TCA) to a final concentration of 10% (w/v). The sample was incubated on ice for 30 min, followed by centrifugation for 2 min at 6700 *g* and the pellet washed twice with cold acetone to remove traces of TCA. The pellet was suspended in 350 µL of Buffer E (Tris-HCl 200

mM, 8 urea M, pH 8.0) and equilibrated at 25 °C for 5 min. To each reduced sample, 0.88 µL of 2-mercaptoethanol were added.

DTNB assay of heat stressed protein

Isolated wine protein (D from HIC, Fig. S1B) was dissolved in water at a concentration of 50 µM. To 250 µL of protein solution, 250 µL of Buffer C (tartaric acid 10 g/L, ethanol 24%, pH 3.2) was added, for a protein final concentration of 25 µM and a concentration of tartaric acid and ethanol equivalent to a wine model solution (tartaric acid 5 g/L, ethanol 12% w/v). To samples "with SO_2", 2.34 µL of a $NaHSO_3$ 100 mg/mL solution was added, for a final concentration of 300 mg/L total SO_2. The samples were then subjected to a heat stability test followed by dilution with 500 µL of Buffer D. 2-Mercaptoethanol (0.88 µL) was added to reduce samples. After equilibration for 1 h at 25 °C, proteins were precipitated by adding TCA to a final concentration of 10% (w/v). The sample was incubated on ice for 30 min, centrifuged 2 min at 6700 *g* and the pellet washed twice with cold acetone to remove traces of TCA. The pellet was suspended in 350 µL of Buffer E (Tris-HCl 200 mM, 8 M urea, pH 8.0) and equilibrated at 25 °C for 5 min.

The DTNB assay was performed applying 100 µL of sample per well in a 96 well microplate followed by 100 µL of Buffer E and 1.33 µL of DTNB solution (3.96 mg/mL). The plate was shaken, and after 10 min incubation at 25 °C, absorbance at 412 nm was read. A summary of the trial is represented in Table S1.

Size exclusion chromatography

The size exclusion chromatography (SEC) protocol was as follows. Fifty µg of protein (at a concentration of 0.5 mg/mL, with or without heat stress; Table S1) was injected

into an ÄKTA Pure system (GE Healthcare) and fractionated using a Superose 12 10/300 GL column (GE Healthcare) at 25 °C. The mobile phase consisted of 8 M urea, 150 mM NaCl, 50 mM sodium citrate, pH 3.0 at a flow rate of 0.5 mL/min. Running time was 40 min and UV detection at 280 nm was used to monitor the elution profile. The calibration curve was performed using blue dextran, ferritin type 1, bovine serum albumin and cytochrome *c* as standards. The standards were all injected in triplicate starting from 0.5 mg/mL solutions. Data were treated in the UNICORN 6.3 software (GE Healthcare) and posterior analysis of the chromatograms was performed in OriginPro 2016 software (OriginLab).

Analysis of protein secondary structure by circular dichroism

Circular dichroism (CD) spectra were recorded in the UV region, between 190 and 320 nm, three scans per temperature point, with a bandwidth of 1 nm on a Chirascan qCD (Applied Photophysics Ltd., Surrey, UK) with a 0.02 cm path-length quartz cylindrical cell (Helma UK Ltd) using protein concentrations of 0.5 mg/mL. The temperature was adjusted by a TC 125 temperature controller (Quantum Northwest) coupled to the CD equipment. To minimize the interference of tartaric acid in CD spectra, the optically inactive *meso* form of tartaric acid was used. The model solution used in CD trials presented the following composition: 5 g/L *meso*-tartaric acid, 12% (v/v) ethanol, pH 3.2 adjusted with 2 M NaOH.

Dynamic light scattering

Dynamic light scattering (DLS) experiments were conducted on a Horiba SZ-100 Nanoparticle analyzer. A diode-pumped solid-state laser (DPSS) 532 nm, 10 mW Class I laser was used as the light source. Autocorrelation curves were acquired with low noise-to-signal ratio and were analyzed by the equipment software through cumulants expansion, which enables retrieval of the particle average hydrodynamic diameter (Z)

and polydispersity assuming the Stokes–Einstein equation is followed for spherical particles (Laia, Lopez-Cornejo, Costa, d'Oliveira, & Martinho, 1998). All samples were filtered prior to preparation and all glassware was washed with filtered Millipore water to avoid any type of dust contamination. To further increase the signal to noise ratio, the concentration of the protein fractions used in this study was adjusted to 500 mg/L in wine model solution. In this work, in the time-dependent DLS experiment, 30 min of acquisition time was selected for the first and last points (at 25 °C and 15 °C after dissolving the protein aggregates) and 30 s for the remaining period of the trial. The geometry applied was 90º and a Peltier system was employed for temperature control. Size distribution analysis was carried out also with the software provided by the equipment manufacturer. To avoid unnecessary data interpretation, the intensity frequency of the size distributions was selected.

Fluorescence spectroscopy

Fluorescence spectra were recorded on a SPEX Fluorolog-3 Model FL3-22 spectrofluorimeter (Horiba Scientific), with an excitation wavelength of 295 nm which is in the right wing the tryptophan excitation spectra to avoid interference of other aromatic residues present in the proteins. All spectra were corrected with correction functions provided by the supplier following standard procedures. Single sets of measurements were performed in the same experimental session. Emission spectra of control solutions of tryptophan in 0.1 M phosphate buffer pH 7.0 was also recorded as a function of temperature. Measurements were performed in triplicate with different protein samples.

Results and discussion

Isolation, purification and characterization of thaumatin-like proteins extracted from wine

Total Moscatel of Alexandria wine proteins were isolated by strong cation exchange chromatography followed by hydrophobic interaction chromatography (HIC; Fig. S1A and B). All fractions were subjected to heat test in wine model solution containing SO_2 as the critical factor. After the heat stability test, we registered that the fraction which produced higher haze, was fraction D. The fraction most prone to aggregate in the presence of sulfur dioxide corresponds to the major protein fraction, an observation which is in agreement to previously published results (Chagas, Ferreira, Laia, Monteiro, & Ferreira, 2016). Protein forms present in fraction D were further analyzed by LC-MS/MS and named D1 and D2 (Table S2).

The two protein sequences were identified by comparison of multiple alignments of the experimentally obtained peptides by LC-MS/MS with non-redundant protein sequence database (PDB). The sequences given by the analysis using BlastP represent similar proteins and not the actual sequences of the purified proteins since LC-MS/MS data did not provide complete coverage of any sequence. Nevertheless, both proteins presented putative conserved domains from the GH64-TLP-SF superfamily, which indicates they belong to the thaumatin protein family. From now on, we will refer to the D protein fraction as isolated thaumatin-like proteins (iTLP). These data are in accordance with Marangon, Van Sluyter, Haynes, and Waters (2009), who presented a high content of TLP in Semillon wine protein fractionated by HIC.

Role of disulfide bonds on iTLP aggregation in the presence of SO_2

The aggregation of heat stressed HIC main wine protein fraction after addition of SO_2, has been previously described by Chagas, Ferreira, Laia, Monteiro, and Ferreira (2016) using a protein concentration of 100 mg/L and 120 mg/L of total SO_2. To increase the protein signal in the following experiments, protein and sulfur dioxide concentrations were increased 5 fold.

Before starting the heat test represented in Figure 1, the DLS measurement allowed the determination of particles in solution with an average diameter equal to 4.9 nm ± 0.9 nm. From the formula described by Erickson (2009) ($Z_{min} = 0.132\ M^{1/3}$, M is given in Dalton and Z_{min} in nm) for the calculation of the minimal diameter of a sphere, the minimal diameter for iTLP using an average molecular weight of 23.8 kDa (based on data from LC-MS/MS analysis) is 3.8 nm. Proteins are described to typically presenting irregular surfaces, i.e. even those that are approximately spherical will have an average hydrodynamic diameter larger than the Z_{min} (Erickson, 2009). It is therefore plausible to assume 4.9 nm as the average diameter of native non-aggregated iTLP in the model wine solution. Afterwards the solution was subjected to a heat test and the size of the particles subsequently evaluated by DLS. Figure 1 shows the dependence of particle diameter *vs.* time / temperature for the aggregation of iTLP in the presence of SO_2.

When isolated wine TLPs are at 70 °C, they will be mainly unfolded (Falconer, Marangon, Van Sluyter, Neilson, Chan, & Waters, 2010) and consequently will present a high exposure of their hydrophobic side-chains to the buffer. Indeed, during the first 120 min at 70°C the particles presented sizes above 10 μm outside the measurement window of the equipment, with light scattering intensity remaining constant within experimental error, which indicate a large degree of aggregation (triggered by hydrophobic interactions). After decreasing the temperature to 15 °C (the cooling step from 70ºC to 15ºC takes about 3 min), autocorrelation curves were possible to measure

indicating an immediate decrease of the particle size to 2 μm, while light scattering intensity increased by two orders of magnitude. When the protein refolds, there is a lower exposure of the hydrophobic side-chains to the buffer and consequently a lower hydration of the protein. This may explain the rapid increment of the light scattering intensity, immediately after decreasing the system temperature to 15 °C. At later times of the trial (between t = 220 and 240 min), the measured particle size was around 8 μm. The aggregation kinetics acquired during this trial is comparable with the one presented by Chagas, Ferreira, Laia, Monteiro, and Ferreira (2016) using 100 mg/L of isolated wine protein in the presence of SO_2 despite using a higher protein concentration in this present experiment. All this strongly contrasts with the measurements performed in an analogous trial with iTLP in the model wine solution without added SO_2. This measurement revealed a very limited formation of aggregates during the cooling step (compared to the sample with added SO_2) with scattered light intensities comparable to the solvent background.

DLS was also used by other authors to study the aggregation of different isolated wine proteins (with emphasis on thaumatin-like proteins and chitinases) with varying conditions including pH, ionic strength, or sulfate content (Dufrechou, Poncet-Legrand, Sauvage, & Vernhet, 2012; Marangon, Sauvage, Waters, & Vernhet, 2011). A noteworthy result was described by Dufrechou, Sauvage, Bach, and Vernhet (2010) when studying protein aggregation in a Sauvignon wine containing 87 mg/L of total SO_2. The authors showed different protein aggregation kinetics depending on the temperature at which the heat test was performed. Particularly, protein aggregation kinetics after heat test performed at either 60 or 70 °C showed to be very similar to the one represented in Figure 1. In the same study, other wines were also tested showing different aggregation behaviors that were attributed to differences in the wine matrix. We propose now that such variations could also be due to differences in the wines SO_2

content (since there were significant differences on the free SO_2 concentration between the tested wines).

The DLS results obtained in the presence of SO_2 show the influence of this compound on protein refolding during the cooling step, leading to different conformation states that eventually give rise to rather large protein aggregates, which ultimately precipitate. We may infer that SO_2 interferes with the formation of new disulfide bonds based not only on the reducing action of this compound but also based on previously published data about the ability of SO_2 to promote the sulfonation of SH groups (Bailey & Cole, 1959). Direct assessment of such reaction should be followed by other techniques, namely circular dichroism and tryptophan fluorescence spectroscopies.

The aggregation and protein secondary structure modification of iTLP upon heating (with and without SO_2 addition) was further studied by CD and UV-visible spectroscopy. To this end, UV CD spectra and UV-visible spectra of iTLP were simultaneously acquired during a heat gradient, like the one obtained during a normal heat test.

The UV CD spectra of iTLP, at 25 ºC and in the absence of SO_2, showed two positive peaks at 194 and 231 nm and a negative peak at 212 nm. The CD spectra obtained for iTLP in the presence of SO_2 was very similar showing no significant differences. Increasing the temperature from 25 to 70 ºC induced a severe change in the CD spectra regardless of the presence of SO_2. Once more, the CD spectra with and without SO_2 at 70 ^{o}C are very similar. After decreasing the temperature to 15 ºC in the absence of SO_2, a regain of secondary structure was detected, characterized by the reappearance of the 230 nm band and a shift of the minimum ellipticity from 202 to 212 nm (Figure 2A). When compared to the iTLP spectrum obtained at 15 ^{o}C in the presence of SO_2, the clear

peak detected at 230 nm becomes reduced to a shoulder. This is a sign of recovery of secondary structure, although with a different conformation (Figure 2B).

To analyze the secondary structure of the proteins, spectra were deconvoluted using the SELCON3, CONTIN and CDSSRT algorithms present in the Dichroweb portal (Whitmore & Wallace, 2004, 2008). The average results from these algorithms are presented in Figure 2C. The results from the individual algorithms are represented in Table S5. The analysis of the results at 25 ºC suggests that iTLP is characterized by a high content in β-sheets and a lower content in α-helices. Similar results for TLP were reported by Di Gaspero, et al. (2017) and Marangon, Van Sluyter, Waters, and Menz (2014). Addition of SO_2 at 25 ºC resulted in a slight decrease in the overall signal (Figure 2C). Nevertheless, no significant modification of the spectra was detected, meaning that the secondary structure of iTLP was practically unaffected by the presence of SO_2 at 25 ºC.

Analyzing the secondary structure results for iTLP in the presence of SO_2, after heating and cooling, indicates a decrease in the β-sheet content and an increase in the α-helix content when compared to iTLP in the absence of SO_2. In protein F2/4JRU, a thaumatin found in wine, it was shown that one of its domains comprising one loop and two β-strands, is stabilized by two disulfide bonds (Marangon, Van Sluyter, Waters, & Menz, 2014). The same authors also studied two isoforms of VVTL1 protein and showed that both β-strands and α-helices are stabilized by disulfide bonds. Based on our results and on previously published data, we can hypothesize that in the presence of SO_2, formation of both inter and intra molecular disulfide bonds induces not only iTLP aggregation but also a decrease in its β-sheet content followed by an increase of the α-helix content. Thereby, the reaction between iTLP and SO_2 at elevated temperature induces formation of new configuration states of iTLP which will partially precipitate after decreasing the

temperature of the solution, confirming our previously published data (Chagas, Ferreira, Laia, Monteiro, & Ferreira, 2016). The augmented predisposition of α-helix chameleon peptides to aggregate when compared with the same sequence with a β-sheet structure gives support to this insight that an increase of the α-helix content can promote the aggregation propensity of the protein (Kim, Do, Hayden, Teplow, Bowers, & Shea, 2016).

The disappearance of the 230 nm band by the action of temperature or pH on proteins has already been reported by Hider, Kupryszewski, Rekowski, and Lammek (1988) when studying the conformation of α-neurotoxins of elapid venoms and neurohypophyseal hormones. These authors showed that closely related conformers of oxytocin differing in the chirality of their disulfide bridges presented different signals in the 220 – 230 nm region. This is in accordance with previous observations showing that the 220 – 230 nm region is critically dependent on the disulfide torsion angles (Kahn, 1979). A change in disulfide bonds can induce a loss in signal in that region. Upon refolding, formation of a different pattern of disulfide bonds can change the torsion angles of these bonds (due to the non-native conformation of the protein), resulting in a significantly different signal at 220 – 230 nm for iTLP in the presence of SO_2 after decreasing the temperature to 15 ºC. In the absence of SO_2, a reappearance of this signal was noted for iTLP, most probably corresponding to reformation of the original pattern of disulfide bonds within the protein.

Changes in sample turbidity during this heat gradient were registered by monitoring the changes in the UV-visible absorption spectra at 540 nm (Figure S2). The most noticeable difference among samples corresponds to the turbidity that develops upon cooling from 70 to 15 ºC of the iTLP sample in the presence of added SO_2. This indicates the formation of protein aggregates followed by partial precipitation.

Further evidence about the involvement of disulphide bonds may be gathered from fluorescence measurements. Tryptophan fluorescence is known to be quenched by nearby disulphide bonds through electron-transfer processes (Cowgill, 1967). A scrambling effect of disulphide bonds upon cooling in the presence of SO_2 would presumably lead to longer average distances which should reduce this quenching effect. Under these conditions, fluorescence intensity should increase. This effect should not happen in the absence of SO_2 since the protein seems to refold to its original state. Fluorescence measurements confirmed this effect, as shown in Figure 3. During heating, in the sample without SO_2 (Figure 3A), fluorescence intensity increases slightly with a red shift, which reflects mainly the increasing exposure of tryptophan residues. In the presence of SO_2 (Figure 3C) the observed result is the same. The cooling step performed after the heat stress, however, reveals a completely different behaviour between the samples. Without SO_2 (Figure. 3B), the cooling follows the same trend backwards, so that at 15 ºC the tryptophan fluorescence presents only a slight increase compared to the protein at 25 ºC before heat stress. However, in the presence of SO_2 (Figure 3D), spectra shift again to the blue indicating refolding of the protein, but fluorescence intensity shows a 3-fold increase. This increase in Trp fluorescence is an indication that quenching by disulphide bonds is less effective under these conditions. A similar phenomenon was reported for a cutinase reduced by the addition of dithiothreitol (DTT), confirming the proximity between Trp residues and the disulphide bridge observed in native cutinase (Neves-Petersen, Gryczynski, Lakowicz, Fojan, Pedersen, Petersen, et al., 2002). This indicates that if a different pattern of S-S bonds is formed in iTLP, it will be at longer distances from Trp residues, at positions which differ from those in the native protein. This effect suggests that SO_2 induces conformational changes also at the level of iTLP Trp residues, and this occurs as iTLP self-aggregates.

Structural studies on iTLP aggregates

To study iTLP aggregates formed after heat stress, their solubility was tested in a series of buffers with varying salt concentrations, denaturant concentrations and pH. The iTLP aggregate-containing protein pellet could be fully dissolved in two different buffers; buffer A (8 M urea, 200 mM NaCl, 30 mM sodium citrate, pH 3.0) and buffer B (4% w/v SDS, 200 mM NaCl, 200 mM Tris-HCl, pH 8.0). Chagas, Ferreira, Laia, Monteiro, and Ferreira (2016) proposed that SO_2-modulated aggregation of a main wine protein fraction could be attributed to formation of new intra- and interprotein disulfide bonds, which could eventually evolve to and/or promote subsequent protein aggregation. Solubilization of the protein pellet in buffer A or buffer B provided new insights about the nature of the aggregates, demonstrating full solubilization of iTLP aggregates in a denaturing, high ionic strength, non-reducing medium. Since the pellet is insoluble in 1 M NaCl (excluding possible ionic interactions) but soluble in buffer A or B, we may conclude that hydrophobic interactions also participate in the aggregation phenomena in addition to disulfide bond scrambling.

To detect the presence of other possible covalently-bound, iTLP-containing species in solution, i.e. other than the ones upheld by non-covalent binding (mainly hydrophobic and ionic interactions), size-exclusion chromatography of iTLP solubilized aggregates was performed. To achieve a good fractionation, buffer A was selected as mobile phase to ensure full solubilization of iTLP aggregates. A similar approach was reported by Chow, Kurt, Murphy, and Cavagnero (2006) for characterizing apomyoglobin self-associated species in urea solutions. The chromatograms of iTLP dissolved in mobile phase and of iTLP after heat stability test in the absence or presence of SO_2 are represented in Figure 4.

The molecular weights of the different molecular species present in the non-reducing buffer (Figure 4A) was determined (Table S3). iTLP presented a single peak with a retention volume of 13.83 mL, corresponding to an estimated molecular weight of 21.1 kDa. Similarly, the same fraction after heat stress without addition of SO_2 presented a molecular weight of 21.4 kDa, showing that heat treatment has no impact on either iTLP size or aggregation in the absence of SO_2.

The chromatographic profile of heat stressed iTLP with added SO_2 shows the presence of two main peaks, one with a retention volume of 11.44 mL, the other with 12.8 mL, corresponding to 37.4 and 79.4 kDa, respectively. This can be related to formation of disulfide bond-linked dimeric and tetrameric molecular species when the protein is heat stressed in the presence of SO_2. The chromatographic profiles of the supernatants collected from the iTLP heat stressed samples (Figure 4) show that there are no detectable protein peaks left in soluble form after iTLP heat stress. To further analyze the chromatographic profile of iTLP aggregate units, statistical analysis was performed (Figure 4C).

After fitting the chromatogram, it is possible to differentiate three different peaks corresponding to monomeric iTLP and to iTLP-covalently linked tetrameric and dimeric species. Considering that the number of Trp, Tyr and Phe residues remain constant during the experiment, we can calculate the relative amount of molecules of the distinct species by dividing the peak area for each species by the number of monomers believed to be present in the different species (division by two in the case of dimers, and by four in the case of tetramers). Analyzing the number of molecules present in solution reveals that there are 70.4 % of iTLP monomers, 24.4 % of dimers and 5.2 % of tetramers. Further analysis is described in Table S4. Thus, most of the

molecules in solution are monomers that self-aggregated via hydrophobic and electrostatic interactions.

Samples identical to those used for Figure 4A were reduced using TCEP and subsequently analyzed by SEC, as represented in Figure 4B. After reducing the samples and superimposing the different chromatograms, a single main fraction is present in all samples that corresponds to monomeric iTLP (21.1 kDa). There is a shift in the retention volume of all samples due to a change in the apparent molecular weight of unfolded iTLP. Nevertheless, considering that native iTLP in model wine solution is exclusively composed of monomers, we may infer the presence of monomeric species in the other samples by the values of peak retention. The presence of lower molecular weight polypeptides was also detected in the reduced heat stressed iTLP with or without SO_2 addition, possibly related to protein degradation during heat treatment.

The 'dimers' and 'tetramers' present in the nonreduced, heat stressed iTLP treated with SO_2 do not appear in the chromatogram of the same sample reduced with TCEP. This can lead to the conclusion that the 'dimers' and 'tetramers' can self-aggregate among themselves and/or with monomers, in a process involving not only hydrophobic and electrostatic interactions, but also scrambled intramolecular dissulfide bridges. Intermolecular dissulfide bridges do participate in the process of 'dimer' and 'tetramer' formation. Is is noteworthy to mention that we failed to detect the presence of iTLP 'trimers'.

In several proteins, intramolecular disulfide bonds are required for folding into native structures and contribute to increase protein thermal stability (Trivedi, Laurence, & Siahaan, 2009). Reduction followed by aberrant scrambled disulfide bond formation results in protein misfolding (Sevier & Kaiser, 2002). Hoffmann and vanMil (1997)

reported that thiol/disulfide exchange reactions lead to formation of aggregates of disulfide-linked β-lactoglobulin monomers together with non-covalent interactions.

Studying the reaction of DTNB with the sulfhydryl groups present in iTLP revealed the occurrence of free sulfhydryl groups after iTLP reduction and allowed studying the effect of high temperature. A specific protocol had to be optimized for the analysis of iTLP aggregates.

iTLP does not have any of its 16 Cys residues with free sulfhydryl groups, since they all participate in eight disulfide bridges (based on available PDB data about VVTL1). After statistical analysis, we can conclude that iTLP, heat stressed iTLP and heat stressed iTLP in the presence of SO_2, do not present a significant difference in their number of free sulfhydryl groups (Figure 5).

If each one of the 16 iTLP Cys residues is bound to another Cys residue, we can say that there are no free sulphydryl groups in either native iTLP or heat stressed iTLP in the absence or presence of SO_2. After reduction with TCEP, there is a signal increase due to the expected reduction of disulfide bounds. In these conditions, no significant differences were observed among the three samples, showing all sulfhydryl groups are in free form. Overall, these results show formation of iTLP 'dimers' and 'tetramers' by intermolecular disulfide bridges, as well as the absence of free sulphydryl groups in the three samples examined. Furthermore, iTLP aggregates involve disulfide bridge scrambling among different iTLP molecules and the consequent formation of new disulfide bridges, leaving no free sulphydryl groups.

Updated mechanism for wine protein haze formation

Based on the recently revised unfolding and aggregation mechanisms of heat-unstable proteins in wine suggested by Van Sluyter, et al. (2015), on the role reported for SO_2 in the chemical build-up of protein aggregates in wines by Chagas, Ferreira, Laia, Monteiro, and Ferreira (2016), and on the results described in this work, we propose an update for the mechanism responsible for protein haze formation in white wines (Figure 6).

Vinification can be envisaged as a 'purification strategy' for grape pathogenesis-related (PR) proteins (Ferreira, Monteiro, Piçarra-Pereira, & Teixeira, 2004). Following winemaking, the proteins that subsist are stable and folded. To trigger the aggregation and precipitation of these proteins, they must undergo an unfolding process in the presence of SO_2. The unfolding of these proteins can occur mainly due to exposure to high temperatures during storage or transportation of the wine. During this unfolding process, hydrophobic pockets of the proteins will be exposed to the surrounding aqueous environment and the SO_2 will reduce disulfide bonds and bind to TLP sulphydryl groups (Chagas, Ferreira, Laia, Monteiro, & Ferreira, 2016; Lundblad, 2014). Upon cooling, these unstable proteins, mainly TLPs, will form a different pattern of S-S' bonds (resulting from the partial sulfonation of cysteine residues), which will result in altered protein configurations, inducing the formation of covalently bound protein 'dimers' and 'tetramers', thus restraining TLP from refolding to its native state while leaving hydrophobic patches facing outwards. As a result, incorrectly folded TLP 'monomers', 'dimers' and 'tetramers' will self-aggregate during the refolding process. These aggregates are maintained mainly by hydrophobic interactions and may be modulated by other factors, including pH, ionic strength, organic acids or by other organic compounds that can bind/interact with the proteins (Batista, Monteiro, Loureiro, Teixeira, & Ferreira, 2010; Chagas, Lourenco, Monteiro, Ferreira, & Ferreira, 2017; Marangon, Van Sluyter, Waters, & Menz, 2014; Marangon, Vincenzi, Lucchetta, &

Curioni, 2010). These polypeptide species will interact to form high molecular weight, insoluble protein aggregates, responsible for a visible haze in the wine following a nucleation growth kinetics (Chagas, Ferreira, Laia, Monteiro, & Ferreira, 2016).

Marangon, et al., (2014) showed that different wine isolated TLP isoforms presented different haze formation behaviour after heat stress. Performing a BlastP analysis of the main protein identified in this work (AAQ10092.1), we can see that one of the proteins most homologous to ours is protein 4JRU, previously crystalized by Maragon et al., (2014). This TLP isoform was described to be the most prone to aggregate after heat stress in the presence of sulfate (added in the form of K_2SO_4). These observations emphasize that; 1) this class of proteins can be the main responsible for protein haze phenomenon, 2) wines with high content of this protein can be more heat unstable, exacerbating the effect of the modulating factors.

Conclusions

The basic factors and conditions for wine TLP aggregation, when subjected to a heat stress in the presence of SO_2, are essentially hydrophobic interactions and formation of a new pattern of covalent bonds by disulfide bridge scrambling. Analysis of TLP secondary structure confirmed that this protein assumes different conformations upon cooling (after a heat stress), depending on the presence or not of SO_2. It also allowed detection of changes in the pattern of the TLP disulfide bridges, indicating a possible torsion of the angle of these bonds which can be related to the formation of different inter- and intramolecular disulfide bridges.

The chemical mechanism underlying the interaction between wine proteins and sulfur dioxide was further elucidated and is supposedly the general mechanism occurring in

unstable commercial wines containing added SO_2. Despite the important and putatively essential influence of SO_2 on wine protein aggregation, this phenomenon continues to be wine-dependent and modulated by the wine matrix.

Acknowledgments

We would like to thank Ana Lourenço for all the help in the elaboration of this work, to Sara Monteiro and Luis Batista for all the work developed during the first years of studying this problem in our laboratory and to Elisabete Ferreira for the help with the circular dichroism analysis. This work was supported by the Associate Laboratory for Green Chemistry LAQV, which is financed by national funds from FCT/MEC (UID/QUI/50006/2013) and co-financed by the ERDF under the PT2020 Partnership Agreement (POCI-01-0145-FEDER - 007265) and through the research unit UID/AGR/04129/2013 (LEAF). This work was also supported by Fundação para a Ciência e a Tecnologia (FCT) under the PhD grant SFRH/BD/84749/2012.

Supporting information

Summary of the DTNB assay in Table S1. Supplemental results of protein purification, UV-visible spectroscopy and circular dichroism.

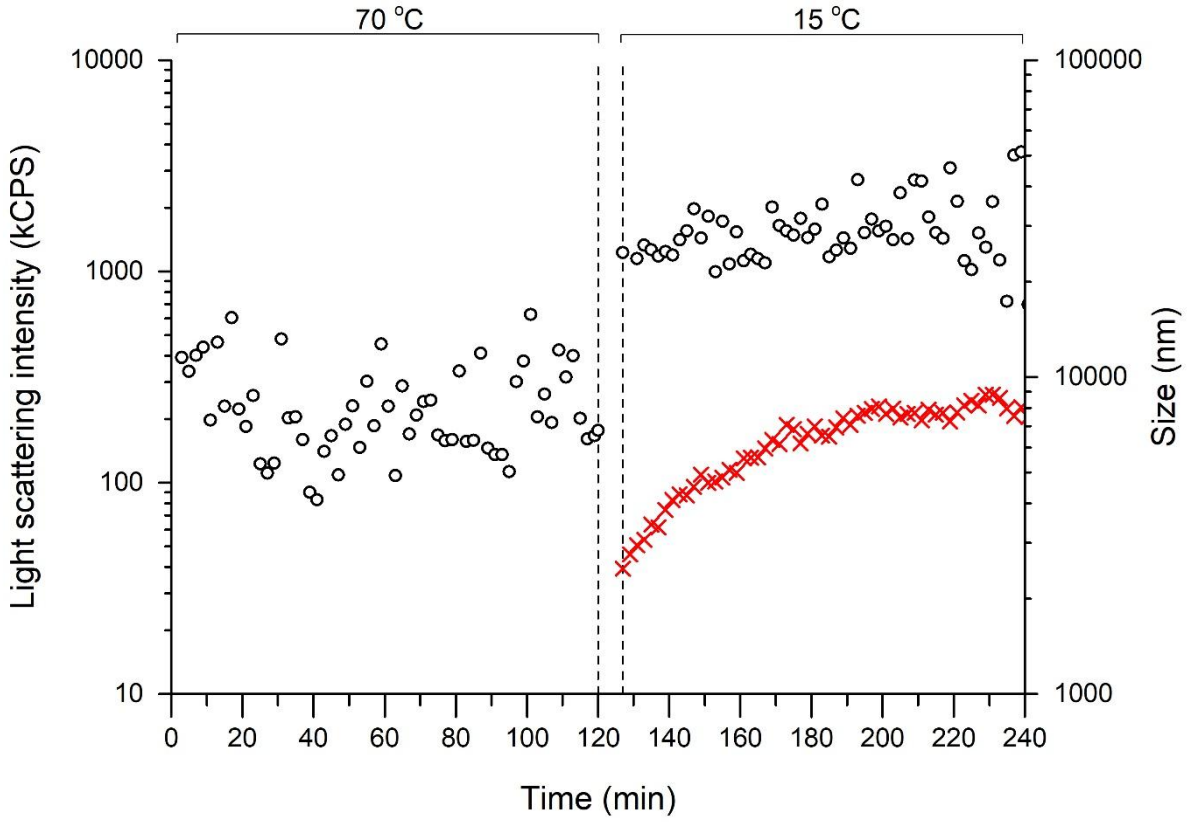

Figure 1 – Dependence of particle diameter on time and temperature for the aggregation of iTLP (at 500 mg L^{-1}) in model wine solution containing SO_2 (at 600 mg L^{-1}). The count rate is represented by (**o**) and the measured diameter by (**x**). The time required to decrease the temperature from 70 to 15 °C (i.e. 8 min) is represented by the vertical dashed lines.

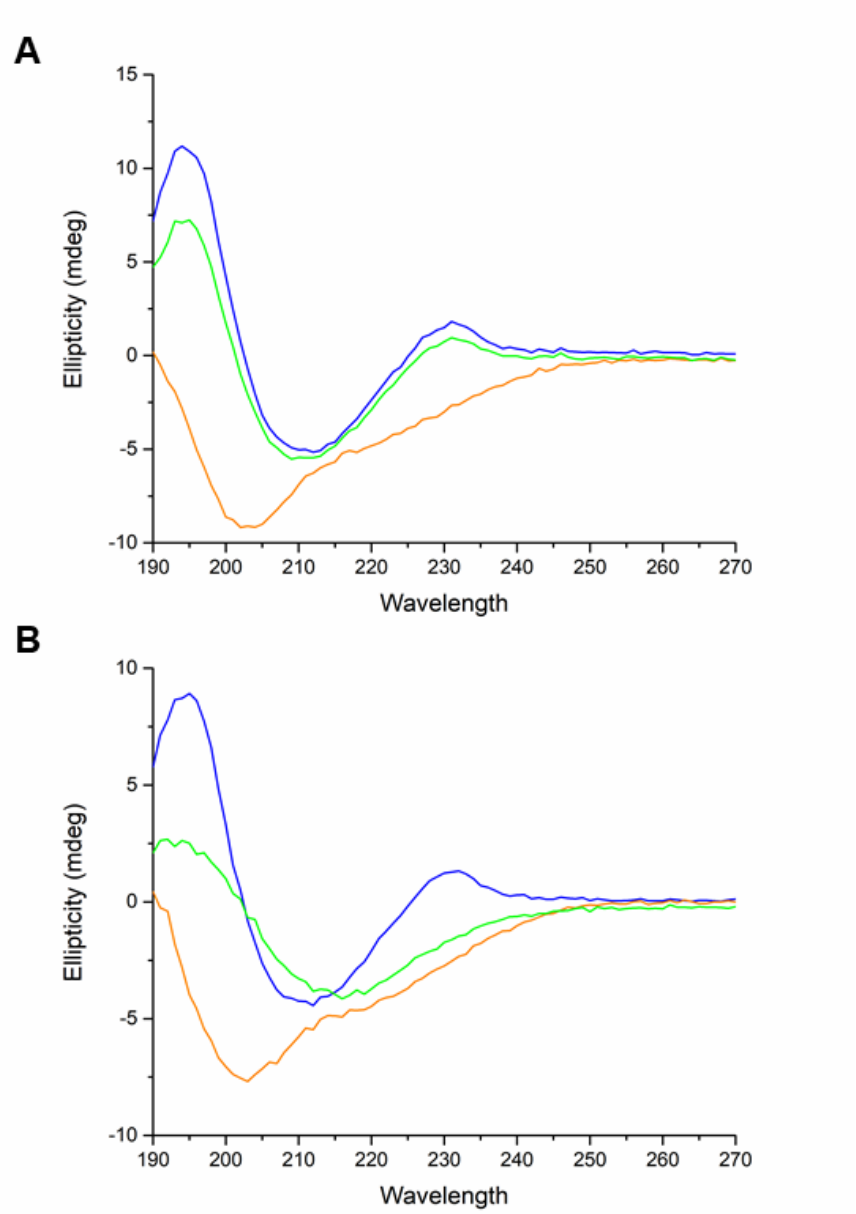

C

		Helix α	Sheet β	Turns	Random Coil
20 °C	iTLP	8.0	41.4	9.7	39.8
	iTLP + SO_2	8.4	42.1	9.6	39.4
70 °C	iTLP	11.6	30.3	14.9	42.2
	iTLP + SO_2	10.5	33.8	14.7	42.6
15 °C	iTLP	9.8	39.3	10.8	39.2
	iTLP + SO_2	21.2	28.3	11.7	38.5

Figure 2 – **A)** CD spectra of iTLP (at 500 mg L^{-1}) in model wine solution (absence of SO_2). **B)** CD spectra of iTLP in model wine solution in the presence of SO_2 (at 600 mg

L^{-1}). Spectra corresponding to temperatures of 25 ºC, 70 ºC and 15 ºC are represented in blue, orange and green, respectively. **C)** Secondary structure analysis of iTLP (with and without added SO_2) by the deconvolution of CD spectra with the algorithms SELCON3, CONTIN and CDSSTR. The values presented in this table correspond to the averages of the results acquired by the different algorithms per each point represented as percentage. The dataset used in these analyses were the SP175 available in the Dichroweb portal. The individual values per each algorithm are available in Table S5.

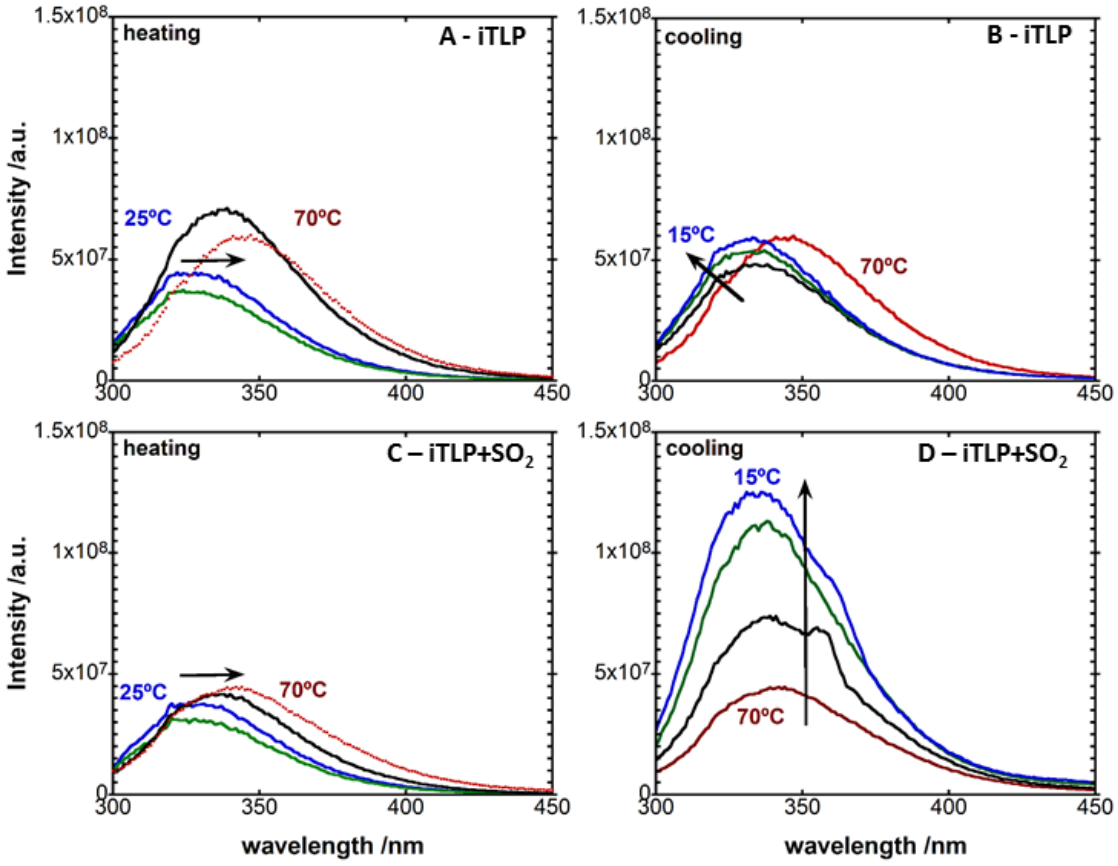

Figure 3 - Tryptophan emission intensity of **A)** and **B)** iTLP (100 mg L^{-1} in model wine solution in the absence of SO_2) and **C)** and **D)** iTLP (100 mg L^{-1} in model wine solution) in the presence of SO_2 (120 mg/L total SO_2). **A)** and **C)**, heating: blue 25 ºC, green 40

ºC, black 60 ºC and red 70 ºC; **B)** and **D)**, cooling (following heat stress represented in **A)** and **C**): red 70 ºC, black 50 ºC, green 25 ºC and blue 15 ºC). Black arrows represent the shift of the curves with time and temperature.

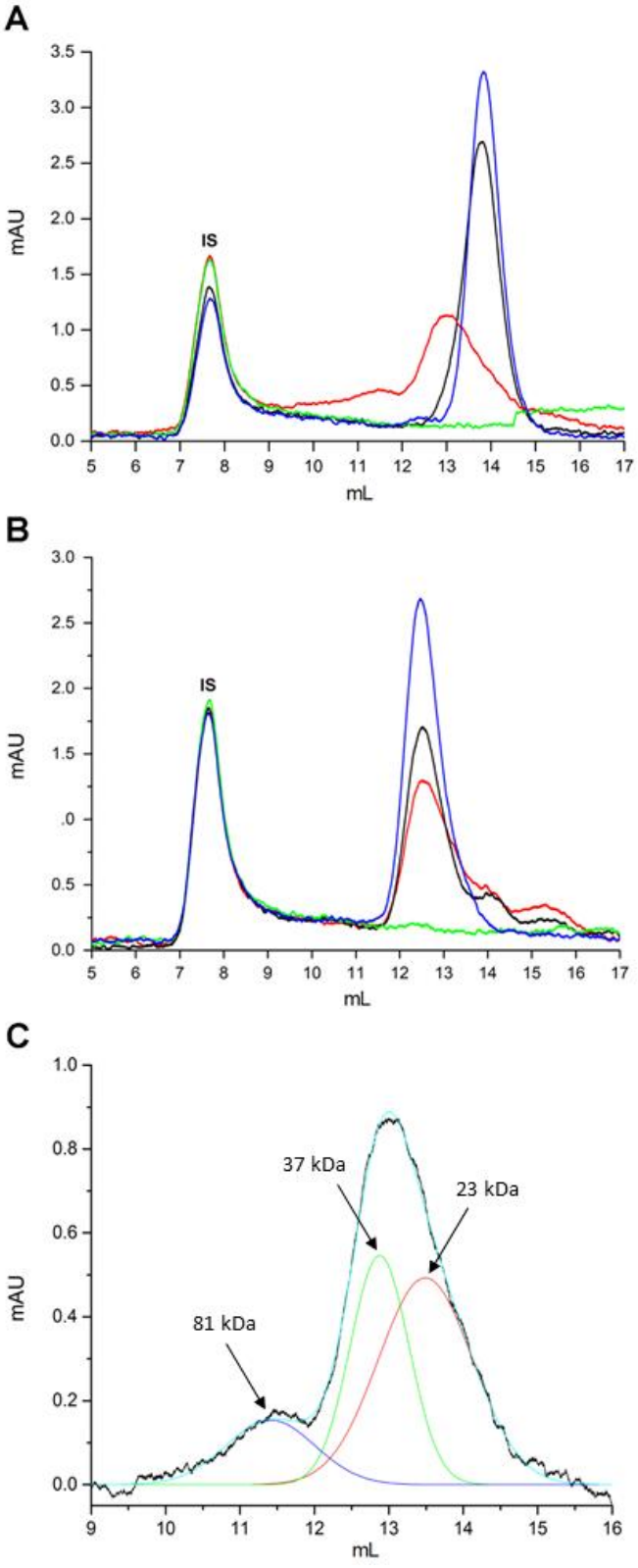

Figure 4 – Size-exclusion chromatogram of non-reduced (**A**) and reduced (**B**) iTLP dissolved in MWS (→), iTLP after heat stability test (absence of SO_2) (→), pellet (→ and

supernatant (→ of iTLP after heat stability test (presence of SO_2) in buffer A. First peak at 7.9 mL corresponds to blue dextran used as internal standard (IS). **C**) Experimental data (extracted from **A**) and corresponding fitting of the chromatographic profile of the heat stressed iTLP in the presence of SO_2 (baseline corrected). Multi-peak Gaussian analysis of the chromatograms is represented by the different fit peaks represented in the figure: iTLP after heat stability test (presence of SO_2) (→, fit peak 1 (→, fit peak 2 (→, fit peak 3 (→ and cumulative fit peak (→.

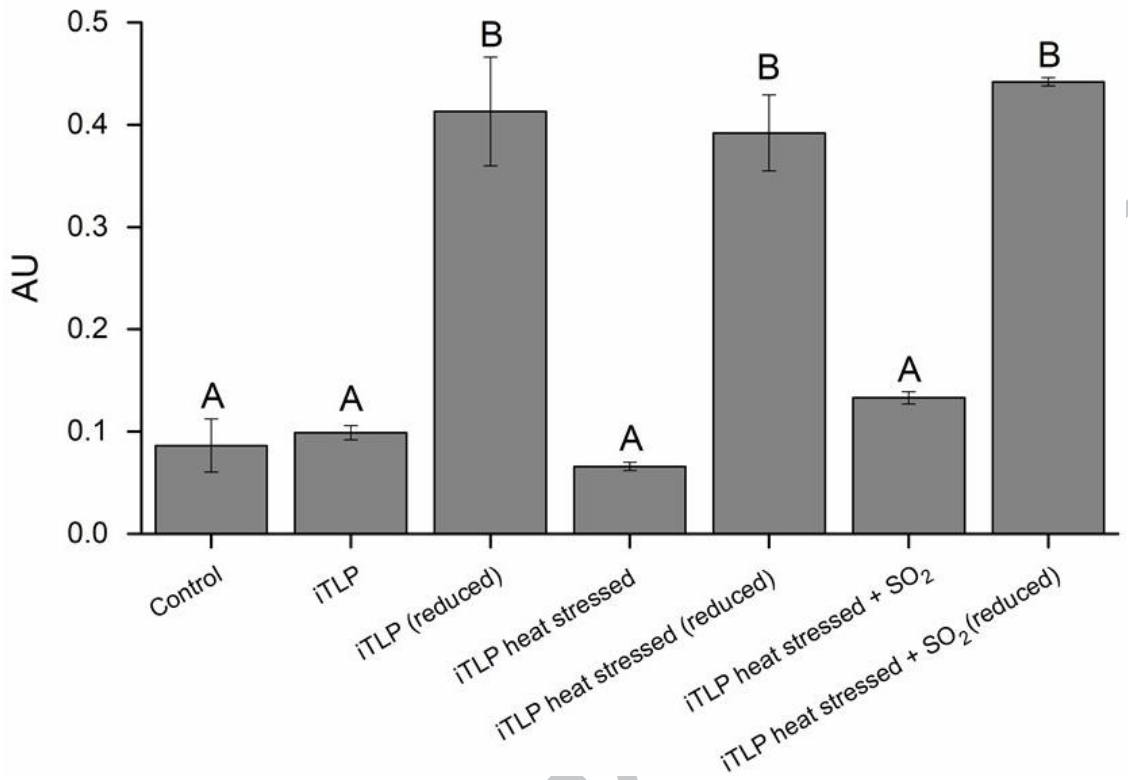

Figure 5 – Reaction of iTLP with DTNB reagent in buffer E containing 200 mM Tris-HCl, 8 M urea, pH 8.0. Control corresponds to the assay performed in the absence of protein. Mean values not sharing the same letter are significantly different (OneWay-ANOVA, Tukey HSD, $P < 0.05$).

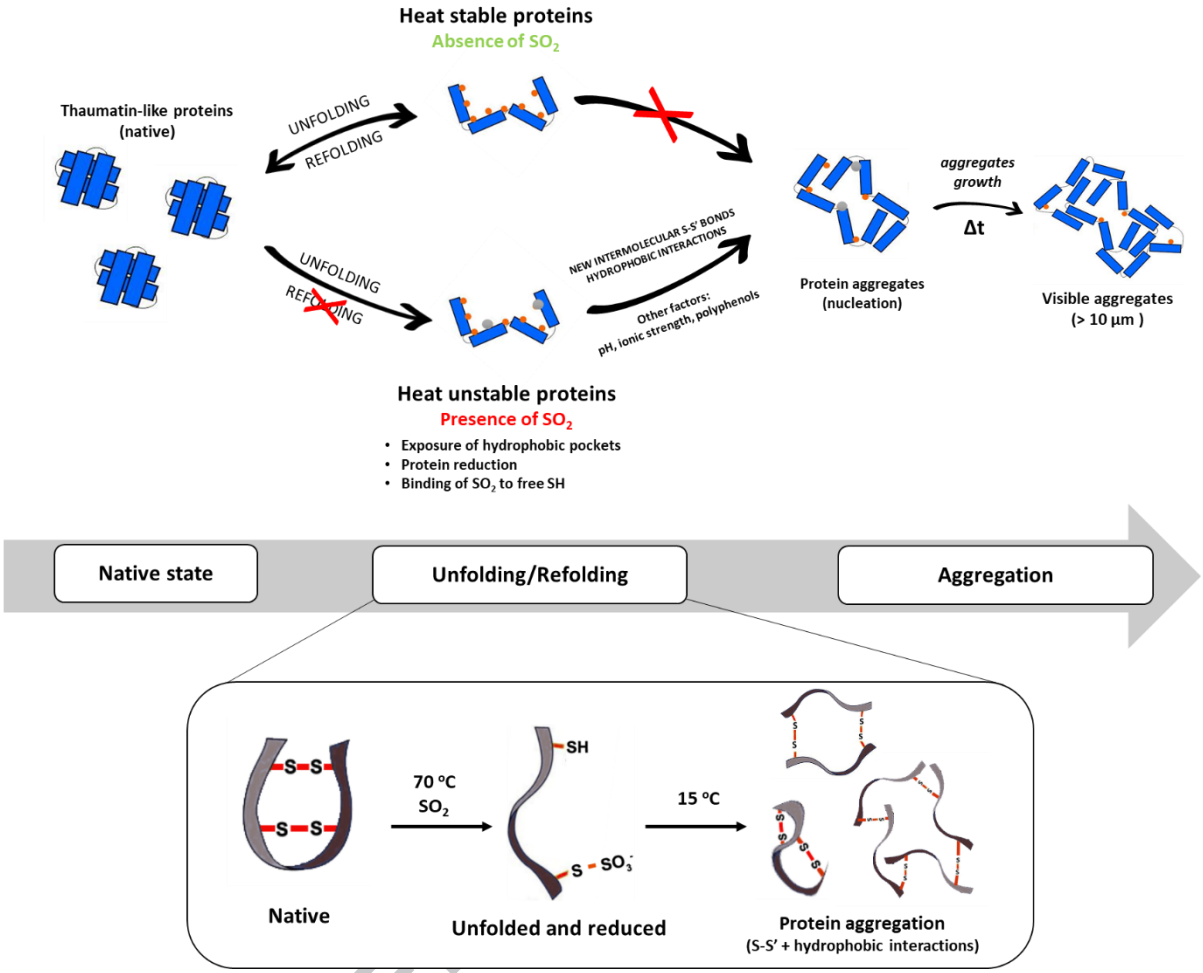

Figure 6 – Updated model for the protein haze development mechanism in white wine.

TOC Graphic

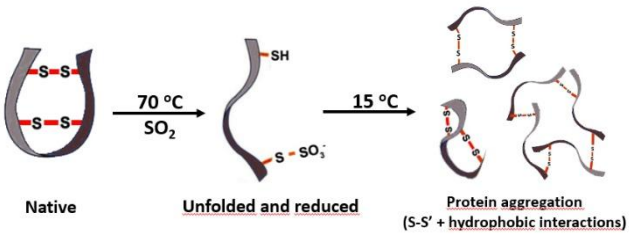

Bailey, J. L., & Cole, R. D. (1959). Studies on the Reaction of Sulfite with Proteins. *Journal of Biological Chemistry, 234*(7), 1733-1739.

Batista, L., Monteiro, S., Loureiro, V. B., Teixeira, A. R., & Ferreira, R. B. (2009). The complexity of protein haze formation in wines. *Food Chemistry, 112*(1), 169-177.

Batista, L., Monteiro, S., Loureiro, V. B., Teixeira, A. R., & Ferreira, R. B. (2010). Protein haze formation in wines revisited. The stabilising effect of organic acids. *Food Chemistry, 122*(4), 1067-1075.

Chagas, R., Ferreira, L. M., Laia, C. A., Monteiro, S., & Ferreira, R. B. (2016). The challenging SO2-mediated chemical build-up of protein aggregates in wines. *Food Chemistry, 192*, 460-469.

Chagas, R., Lourenco, A. M., Monteiro, S., Ferreira, R. B., & Ferreira, L. M. (2017). Is caffeic acid, as the major metabolite present in Moscatel wine protein haze hydrolysate, involved in protein haze formation? *Food Research International, 98*, 103-109.

Chow, C., Kurt, N., Murphy, R. M., & Cavagnero, S. (2006). Structural Characterization of Apomyoglobin Self-Associated Species in Aqueous Buffer and Urea Solution. *Biophysical Journal, 90*(1), 298-309.

Ciaccio, N. A., & Laurence, J. S. (2009). Effects of Disulfide Bond Formation and Protein Helicity on the Aggregation of Activating Transcription Factor 5. *Molecular Pharmaceutics, 6*(4), 1205-1215.

Cowgill, R. W. (1967). Fluorescence and Protein Structure .11. Fluorescence Quenching by Disulfide and Sulfhydryl Groups. *Biochimica Et Biophysica Acta, 140*(1), 37-&.

Creamer, L. K., Bienvenue, A., Nilsson, H., Paulsson, M., van Wanroij, M., Lowe, E. K., Anema, S. G., Boland, M. J., & Jimenez-Flores, R. (2004). Heat-induced redistribution of disulfide bonds in milk proteins. 1. Bovine beta-lactoglobulin. *J Agric Food Chem, 52*(25), 7660-7668.

Di Gaspero, M., Ruzza, P., Hussain, R., Vincenzi, S., Biondi, B., Gazzola, D., Siligardi, G., & Curioni, A. (2017). Spectroscopy reveals that ethyl esters interact with proteins in wine. *Food Chemistry, 217*, 373-378.

Dufrechou, M., Poncet-Legrand, C., Sauvage, F. X., & Vernhet, A. (2012). Stability of White Wine Proteins: Combined Effect of pH, Ionic Strength, and Temperature

on Their Aggregation. *Journal of Agricultural and Food Chemistry, 60*(5), 1308-1319.

Dufrechou, M., Sauvage, F. X., Bach, B., & Vernhet, A. (2010). Protein aggregation in white wines: influence of the temperature on aggregation kinetics and mechanisms. *J Agric Food Chem, 58*(18), 10209-10218.

Dufrechou, M., Vernhet, A., Roblin, P., Sauvage, F. X., & Poncet-Legrand, C. (2013). White wine proteins: how does the pH affect their conformation at room temperature? *Langmuir, 29*(33), 10475-10482.

Erickson, H. P. (2009). Size and Shape of Protein Molecules at the Nanometer Level Determined by Sedimentation, Gel Filtration, and Electron Microscopy. *Biological Procedures Online, 11*(1), 32-51.

Falconer, R. J., Marangon, M., Van Sluyter, S. C., Neilson, K. A., Chan, C., & Waters, E. J. (2010). Thermal stability of thaumatin-like protein, chitinase, and invertase isolated from Sauvignon blanc and Semillon juice and their role in haze formation in wine. *J Agric Food Chem, 58*(2), 975-980.

Ferreira, R. B., Monteiro, S. S., Piçarra-Pereira, M. A., & Teixeira, A. R. (2004). Engineering grapevine for increased resistance to fungal pathogens without compromising wine stability. *Trends in Biotechnology, 22*(4), 168-173.

Ferreira, R. B., Piçarra-Pereira, M. A., Monteiro, S., Loureiro, V. l. B., & Teixeira, A. R. (2001). The wine proteins. *Trends in Food Science & Technology, 12*(7), 230-239.

Garde-Cerdán, T., López, R., Garijo, P., González-Arenzana, L., Gutiérrez, A. R., López-Alfaro, I., & Santamaría, P. (2014). Application of colloidal silver versus sulfur dioxide during vinification and storage of Tempranillo red wines. *Australian Journal of Grape and Wine Research, 20*(1), 51-61.

Hider, R. C., Kupryszewski, G., Rekowski, P., & Lammek, B. (1988). Origin of the positive 225-230 nm circular dichroism band in proteins. Its application to conformational analysis. *Biophys Chem, 31*(1-2), 45-51.

Hoffmann, M. A. M., & vanMil, P. J. J. M. (1997). Heat-induced aggregation of beta-lactoglobulin: Role of the free thiol group and disulfide bonds. *Journal of Agricultural and Food Chemistry, 45*(8), 2942-2948.

Hsu, J. C., & Heatherbell, D. A. (1987). Isolation and Characterization of Soluble-Proteins in Grapes, Grape Juice, and Wine. *American Journal of Enology and Viticulture, 38*(1), 6-10.

Jaeckels, N., Meier, M., Dietrich, H., Will, F., Decker, H., & Fronk, P. (2016). Influence of polysaccharides on wine protein aggregation. *Food Chemistry, 200*, 38-45.

Kahn, P. C. (1979). The interpretation of near-ultraviolet circular dichroism. *Methods Enzymol, 61*, 339-378.

Kim, B., Do, T. D., Hayden, E. Y., Teplow, D. B., Bowers, M. T., & Shea, J.-E. (2016). Aggregation of Chameleon Peptides: Implications of α-Helicity in Fibril Formation. *The Journal of Physical Chemistry B, 120*(26), 5874-5883.

Laia, C. A. T., Lopez-Cornejo, P., Costa, S. M. B., d'Oliveira, J., & Martinho, J. M. G. (1998). Dynamic light scattering study of AOT microemulsions with nonaqueous polar additives in an oil continuous phase. *Langmuir, 14*(13), 3531-3537.

Lundblad, R. (2014). *Chemical Reagents for Protein Modification, Fourth Edition*: CRC Press.

Marangon, M., Sauvage, F. X., Waters, E. J., & Vernhet, A. (2011). Effects of Ionic Strength and Sulfate upon Thermal Aggregation of Grape Chitinases and

Thaumatin-like Proteins in a Model System. *Journal of Agricultural and Food Chemistry, 59*(6), 2652-2662.

Marangon, M., Stockdale, V. J., Munro, P., Trethewey, T., Schulkin, A., Holt, H. E., & Smith, P. A. (2013). Addition of Carrageenan at Different Stages of Winemaking for White Wine Protein Stabilization. *Journal of Agricultural and Food Chemistry, 61*(26), 6516-6524.

Marangon, M., Van Sluyter, S. C., Haynes, P. A., & Waters, E. J. (2009). Grape and wine proteins: their fractionation by hydrophobic interaction chromatography and identification by chromatographic and proteomic analysis. *J Agric Food Chem, 57*(10), 4415-4425.

Marangon, M., Van Sluyter, S. C., Waters, E. J., & Menz, R. I. (2014). Structure of haze forming proteins in white wines: Vitis vinifera thaumatin-like proteins. *PLoS One, 9*(12), e113757.

Marangon, M., Vincenzi, S., Lucchetta, M., & Curioni, A. (2010). Heating and reduction affect the reaction with tannins of wine protein fractions differing in hydrophobicity. *Analytica Chimica Acta, 660*(1–2), 110-118.

Neves-Petersen, M. T., Gryczynski, Z., Lakowicz, J., Fojan, P., Pedersen, S., Petersen, E., & Bjorn Petersen, S. (2002). High probability of disrupting a disulphide bridge mediated by an endogenous excited tryptophan residue. *Protein Sci, 11*(3), 588-600.

Pocock, K. F., Alexander, G. M., Hayasaka, Y., Jones, P. R., & Waters, E. J. (2007). Sulfate - a candidate for the missing essential factor that is required for the formation of protein haze in white wine. *Journal of Agricultural and Food Chemistry, 55*(5), 1799-1807.

Rombouts, I., Lagrain, B., Scherf, K. A., Lambrecht, M. A., Koehler, P., & Delcour, J. A. (2015). Formation and reshuffling of disulfide bonds in bovine serum albumin demonstrated using tandem mass spectrometry with collision-induced and electron-transfer dissociation (vol 5, 12210, 2015). *Sci Rep, 5*.

Sevier, C. S., & Kaiser, C. A. (2002). Formation and transfer of disulphide bonds in living cells. *Nature Reviews Molecular Cell Biology, 3*(11), 836-847.

Shimada, K., & Cheftel, J. C. (1989). Sulfhydryl group/disulfide bond interchange reactions during heat-induced gelation of whey protein isolate. *Journal of Agricultural and Food Chemistry, 37*(1), 161-168.

Trivedi, M. V., Laurence, J. S., & Siahaan, T. J. (2009). The Role of Thiols and Disulfides on Protein Stability. *Current Protein & Peptide Science, 10*(6), 614-625.

Van der Plancken, I., Van Loey, A., & Hendrickx, M. E. (2005). Changes in sulfhydryl content of egg white proteins due to heat and pressure treatment. *J Agric Food Chem, 53*(14), 5726-5733.

Van Sluyter, S. C., McRae, J. M., Falconer, R. J., Smith, P. A., Bacic, A., Waters, E. J., & Marangon, M. (2015). Wine protein haze: mechanisms of formation and advances in prevention. *J Agric Food Chem, 63*(16), 4020-4030.

Whitmore, L., & Wallace, B. A. (2004). DICHROWEB, an online server for protein secondary structure analyses from circular dichroism spectroscopic data. *Nucleic Acids Res, 32*(Web Server issue), W668-673.

Whitmore, L., & Wallace, B. A. (2008). Protein secondary structure analyses from circular dichroism spectroscopy: methods and reference databases. *Biopolymers, 89*(5), 392-400.